

A Redox-Induced Spin-State Cascade in a Mixed-Valent $\text{Fe}_3(\mu_3\text{-O})$ Triangle

Evgen V. Govor,^[a] Karrar Al-Ameed,^[b,c] Indranil Chakraborty,^[d] Carla S. Coste,^[d] Olena Govor,^[a] Yiannis Sanakis,^{*[e]} John E. McGrady,^{*[b]} Raphael G. Raptis^{*[a]}

Abstract: One-electron reduction of a pyrazolate-bridged triangular $\text{Fe}_3(\mu_3\text{-O})$ core induces a cascade wherein all three metal centers switch from high-spin Fe^{3+} to low-spin $\text{Fe}^{2.66+}$. This hypothesis is supported by spectroscopic data (^1H -NMR, UV-vis-NIR, infra-red, ^{57}Fe -Mössbauer, EPR), X-ray crystallographic characterization of the cluster in both oxidation states and also density functional theory. The reduction induces substantial contraction in all bond lengths around the metal centers, along with diagnostic shifts in the spectroscopic parameters. This is, to the best of our knowledge, the first example of a one-electron redox event causing concerted change in multiple iron centers.

In a series of recent papers, we have highlighted the utility of the 4-nitropyrazolate ($4\text{-NO}_2\text{-pz}$) ligand system in exploring the chemistry of trinuclear clusters of the type $[\text{M}_3(\mu_3\text{-O})(\mu\text{-}4\text{-NO}_2\text{-pz})_6\text{L}_3]^{2-}$, where $\text{M} = \text{Co}^{3+}$ and Fe^{3+} .^[1-3] The carboxylate analogues of these clusters have been explored extensively,^[4-6] but the pyrazolates offer significant advantages in terms of reduced lability and hence reversible electrochemistry, and this has facilitated studies of mixed valence. The magnetic and electron-transfer properties of the all-ferric “basic iron carboxylates”, $[\text{Fe}_3(\mu_3\text{-O})(\mu\text{-RCOO})_6\text{L}_3]^{2-}$, in particular, have been the focus of detailed investigations.^[7-10] The properties of their one-electron reduced counterparts, formally $2\text{Fe}^{3+}\text{Fe}^{2+}$ species, are highly temperature dependent as a result of the transition from valence trapped to fully delocalized regimes. All three Fe centers, however, retain local high-spin configurations across the entire temperature range,^[7-12] as a combined result of the weak field character of the carboxylate ligand and the large electron-electron repulsion in Fe^{3+} : low-spin configurations at Fe^{3+} are in general uncommon.^[13, 14]

Systems that can switch reversibly between two structurally distinct states in response to an external stimulus are promising candidates for the development of new devices, such as sensors

and memory storage media. In this communication we show that switching to a stronger field pyrazolate ligand gives rise to $\text{Fe}_3(\mu_3\text{-O})$ clusters that lie closer to the high-spin/low-spin crossover point. As a result, whilst the all-ferric complex $[\text{Fe}_3(\mu_3\text{-O})(\mu\text{-}4\text{-NO}_2\text{-pz})_6(\text{NCS})_3]^{2-}$, $[\mathbf{1}^{2-}]$, has structural and spectroscopic properties that are characteristic of high-spin Fe^{3+} centers, its one-electron reduced analogue, $[\text{Fe}_3(\mu_3\text{-O})(\mu\text{-}4\text{-NO}_2\text{-pz})_6(\text{NCS})_3]^{3-}$, $[\mathbf{1}^{3-}]$, has all three metal centers in low-spin configurations ($\text{Fe}^{2.66+}$). Remarkably, therefore, a one-electron reduction induces a cascade wherein all three Fe centers undergo a change in spin state. We describe the structural and spectroscopic evidence for this cascade, and use density functional theory to explore its origins. The redox-induced cascade reported for the first time here complements the well-studied temperature-, pressure-, or photochemically-induced high-spin to low-spin transitions commonly observed in mononuclear and polynuclear spin-crossover complexes.^[15]

The reaction of FeCl_3 with excess $4\text{-NO}_2\text{-pzH}$ and $[\text{N}^t\text{Bu}_4][\text{OH}]$ gives the all-ferric $[\text{N}^t\text{Bu}_4]_2[\text{Fe}_3(\mu_3\text{-O})(4\text{-NO}_2\text{-pz})_6\text{Cl}_3]$ compound in 20% yield (S1). Subsequent reaction of this product with $[\text{NH}_4][\text{SCN}]$ results in ligand metathesis and formation of the NCS-terminated analogue, $[\text{N}^t\text{Bu}_4]_2[\text{Fe}_3(\mu_3\text{-O})(\mu\text{-}4\text{-NO}_2\text{-pz})_6(\text{NCS})_3]$, $[\text{N}^t\text{Bu}_4]_2[\mathbf{1}^{2-}]$, a paramagnetic material, as evident by the paramagnetically-shifted ^1H -NMR resonance of pyrazole protons at 30.00 ppm and the EPR signal with $g = 2.00$ (S2). The cyclic voltammogram of this material reveals a single reversible reduction at -0.36 V (vs. Fc^+/Fc , S3), considerably less negative than the corresponding chloride- and bromide-terminated analogues, which show similar processes at -0.70 V and -0.55 V, respectively.^[2, 3] The relatively facile one-electron reduction exhibited by $[\mathbf{1}^{2-}]$ prompted us to attempt to isolate the mixed-valent analogue *via* chemical reduction; reaction with $[\text{N}^t\text{Bu}_4][\text{BH}_4]$ generated a mixed-valence species $[\text{N}^t\text{Bu}_4]_3[\text{Fe}_3(\mu_3\text{-O})(\mu\text{-}4\text{-NO}_2\text{-pz})_6(\text{NCS})_3]$, $[\text{N}^t\text{Bu}_4]_3[\mathbf{1}^{3-}]$, in 80% yield. $[\text{N}^t\text{Bu}_4]_3[\mathbf{1}^{3-}]$ is EPR silent at 4.2 K and the ^1H nmr resonances of its pyrazole protons are found at 7.79 ppm, indicating a diamagnetic mixed-valence species (S4). $[\text{N}^t\text{Bu}_4]_3[\mathbf{1}^{3-}]$ also shows a characteristic intervalence charge transfer (IVCT) band at 9170 cm^{-1} ($\epsilon = 7800\text{ cm}^{-1}\text{ mol}^{-1}\text{ dm}^3$) that is absent in the all-ferric parent compound (S5). Deconvolution of the IVCT manifold reveals two Gaussian bands with λ_{max} of 9080 cm^{-1} and 10140 cm^{-1} , respectively. Analysis of the principal IVCT component by the Hush method^[16] gives a f value of 0.72, corresponding to a strongly delocalized, Robin-Day class-III system.^[17]

^{57}Fe -Mössbauer spectra were recorded in the 4.2 – 300 K range (S6). The 80 K spectrum of $[\text{N}^t\text{Bu}_4]_2[\mathbf{1}^{2-}]$ (Figure 1) is highly characteristic of high-spin ferric ions, with an isomer shift, $\delta = 0.44(1)\text{ mm/s}$ and quadrupole splitting $\Delta E_Q = 1.20(1)\text{ mm/s}$, consistent with high spin Fe^{3+} and similar to those previously reported for the analogous chloro- and bromo-terminated analogues.^[2, 3] A single doublet is also observed for the reduced species $[\text{N}^t\text{Bu}_4]_3[\mathbf{1}^{3-}]$, suggesting that the additional electron is

[a] Dr. E. V. Govor; O. Govor; Prof. Dr. R. G. Raptis
Department of Chemistry and Biochemistry and the Biomedical Sciences Institute, Florida International University
11200 SW 8th Street, Miami, FL 33199, USA.
E-mail: raphael.raptis@fiu.edu

[b] Prof. Dr. J. E. McGrady
Department of Chemistry, South Parks Road, University of Oxford, OX1 3QZ, United Kingdom.
E-mail: john.mcgrady@chem.ox.ac.uk

[c] K. Al-Ameed
Faculty of Science, University of Kufa, Kufa St., Najaf, Iraq.

[d] Dr. I. Chakraborty; C. S. Coste
Department of Chemistry, University of Puerto Rico,
San Juan, PR 00934, USA.

[e] Dr. Y. Sanakis
Institute of Nanoscience and Nanotechnology, NCSR “Demokritos”,
Ag. Paraskevi, 15310 Attiki, Greece.
E-mail: i.sanakis@inn.demokritos.gr

delocalized over all three iron centers. Moreover, both the isomer shift and the quadrupole splitting -- $\delta = 0.27(1)$ mm/s; $\Delta E_Q = 1.02(1)$ mm/s, respectively -- are lower in $[\text{Bu}_4\text{N}]_3[\mathbf{1}^{3-}]$ than in $[\text{Bu}_4\text{N}]_2[\mathbf{1}^{2-}]$, indicating that the local electronic structure at the metal centers is distinctly different. The dramatic -0.17 mm/s decrease of isomer shift observed upon reduction is an unequivocal indication of high-to-low spin electronic reorganization. The Mössbauer parameters of the $\text{Fe}^{2.66+}$ centers in $[\mathbf{1}^{3-}]$ are in agreement with the average values of two low spin- Fe^{3+} and one low spin- Fe^{2+} with a $D_{4h}\text{-N}_6$ coordination environment.^[18] Infra-red spectroscopy (S7) offers further evidence for a distinct change in electronic structure upon one-electron reduction: the characteristic C-N stretching vibration at 2022 cm^{-1} in the all-ferric species shifts to *higher* frequency, 2081 cm^{-1} , in the mixed-valent analogue (only a single C-N band observed in either case). A similar shift in stretching frequencies has been noted for a mononuclear high spin Fe^{3+} /low-spin Fe^{2+} pair.^[19]

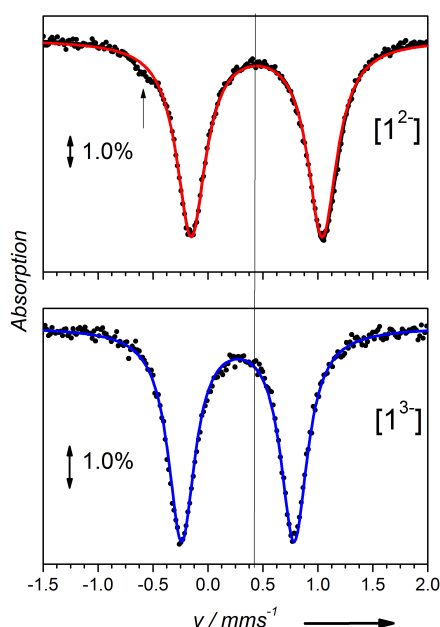


Figure 1. ^{57}Fe -Mössbauer spectra of $[\text{N}^t\text{Bu}_4]_2[\mathbf{1}^{2-}]$ and $[\text{N}^t\text{Bu}_4]_3[\mathbf{1}^{3-}]$ at 80 K. Solid lines are theoretical simulations. The arrow in the spectrum of $[\mathbf{1}^{2-}]$ indicates a shoulder attributed to the low energy line of a doublet arising from 1-2% mononuclear impurity (see S6).

Attempts to solve the crystal structures of $[\text{Bu}_4\text{N}]_2[\mathbf{1}^{2-}]$ and $[\text{Bu}_4\text{N}]_3[\mathbf{1}^{3-}]$ were frustrated by crystallographic disorder problems. However, changing the counterion to $[\text{NEt}_3\text{H}]^+$ gave high-quality crystals of the all-ferric species $[\text{NEt}_3\text{H}]_2[\mathbf{1}^{2-}]$ allowing the determination of its X-ray structure at 210 K. The Fe-O, Fe-N(NCS) and Fe-N(pz) bond lengths of 1.87 Å (av.), 1.99 Å (av.) and 2.12 Å (av.), respectively, are similar to those observed in the chloride- and bromide-capped analogues, and are highly characteristic of high-spin Fe^{III} centers.^[2,3] X-ray quality crystals of the mixed-valent trivalent anion, $[\mathbf{1}^{3-}]$, were obtained by reduction of $[\text{Ph}_4\text{P}]_2[\mathbf{1}^{2-}]$ with cobaltocene, resulting in single crystals of $[\text{PPh}_4][\text{CoCp}_2]_2[\mathbf{1}^{3-}]$. The trianionic complex

(Figure 2) differs from the dianionic one in that all Fe-N and Fe-O bonds are significantly shortened (Table 1), fully consistent with a low-spin configuration. The Co-C distances (2.016 Å , av.) are also consistent with the formulation of the CoCp_2 moieties as cobaltocenium cations. The UV-vis-NIR spectrum of a CH_2Cl_2 solution of $[\text{PPh}_4][\text{CoCp}_2]_2[\mathbf{1}^{3-}]$ showed the diagnostic mixed-valence $[\mathbf{1}^{3-}]$ IVCT band at 9166 cm^{-1} (*vide supra*).

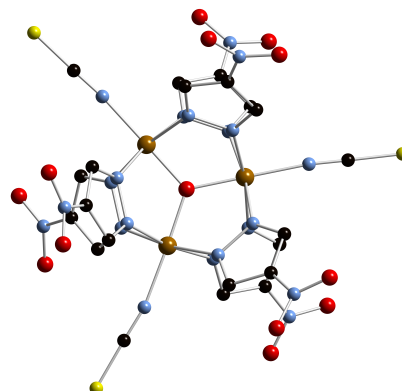


Figure 2. Crystal structure of $[\text{NEt}_3\text{H}]_2[\mathbf{1}^{2-}]$. H atoms are not shown. Color coding: Fe, brown; S, yellow; O, red; N, blue; C, black.

Table 1. Comparison of selected interatomic distances (Å) in $[\text{NEt}_3\text{H}]_2[\mathbf{1}^{2-}]$ at 210 K and $[\text{PPh}_4][\text{CoCp}_2]_2[\mathbf{1}^{3-}]$ at 100 K.

	$[\text{NEt}_3\text{H}]_2[\mathbf{1}^{2-}]$	$[\text{PPh}_4][\text{CoCp}_2]_2[\mathbf{1}^{3-}]$
Fe...Fe	3.2294(6); 3.2613(7)	3.0642(7) – 3.0693(5)
Fe-(μ_3 -O)	1.867(3); 1.882(2)	1.766(2) – 1.774(2)
Fe-N(NCS)	1.990(3); 1.990(4)	1.936(2) – 1.950(2)
Fe-N(pz)	2.111(3) – 2.149(3)	1.946(2) – 1.971(2)

In order to explore the electronic origin of the cascade, and in particular the reasons why one-electron reduction leads to low-spin (L) configurations at all three Fe centers, rather than only one, we have turned to density functional theory (DFT, S9). The absolute determination of the position of equilibrium between high- and low-spin configurations is a very challenging problem for DFT, even in the context of a single metal center, and the utility of various functionals in this context has been debated extensively.^[20] Swart and co-workers have argued that the OPBE functional performs well in spin-crossover systems of iron,^[20b,c] while others favor the use of hybrid functionals, notably Reiher's B3LYP*^[20] and TPSSH^[20k-m] (with 15% and 10% exact Hartree-Fock exchange, respectively). A fuller analysis of the impact of different choices of density functional in this specific system is presented in the supporting information, but we restrict discussion to the OPBE functional in the main body of this work. Polymetallic systems such as those of interest here bring additional complexity for two distinct reasons. First, the electrons in mixed valence species may be localized or partially/fully delocalized (Day-Robin class I/II/III). In systems such as these, where antiferromagnetic coupling dominates, the

wavefunction cannot be described by a single determinant. In principle, the problem could be addressed using multi-configurational approaches such as CASSCF, but the size of the required active space makes such calculations inaccessible at the present time. Advances in density matrix renormalization group (DMRG) techniques may make such calculations possible in the future, but for now the majority of the literature in this field takes advantage of broken-symmetry density functional theory. The broken-symmetry approach allows the spin- α and spin- β electrons to localize in different regions of space, reflecting the localized spin densities prevalent in magnetically coupled systems, and it has been used extensively to disentangle the effects of Heisenberg and double exchange on the ground state properties of iron clusters, for example.^[21] The second issue is that intermediate states can arise where some of the metal centers are in high-spin configurations, some low-spin (denoted HL as distinct from HH or LL). The existence of stable intermediate HL states can give rise to two-step crossover with distinct plateaus in the magnetic susceptibility curves. Bolvin, Kahn and co-workers first explored this issue and developed a phenomenological model wherein the existence of a stable intermediate HL state is detectable only if its energy is lower than the average energy of the HH and LL alternatives.^[22] More recently, Borshch and co-workers have used B3LYP* to study a series of binuclear Fe^{II} complexes with NCX ligands (X = S, Se), confirming that two step crossover is indeed associated with situations where the HL state lies below the HH/LL average.^[23] In subsequent papers the same group have presented detailed analyses of the coordination geometries in a series of bimetallic Fe^{II} complexes, and argued that ligand strain effects are the key to understanding the stability of intermediate HL states.^[24] If the change from H to L at the first center alters the coordination sphere of the second such that the H form is favored (i.e. the ligand field is weakened) then an HL state will be stabilized.

In Figure 3(a), the relative energies of the lowest energy states of $[1^3]$ with three, two, one and zero locally high-spin iron centers (denoted HHH, HHL, HLL and LLL, respectively) are plotted (red line). The corresponding data for a model carboxylate-bridged analogue, $[\text{Fe}_3(\mu_3\text{-O})(\mu\text{-HCOO})_6(\text{NCS})_3]^{3-}$, are also shown for comparison (green line). It is immediately clear from Figure 3(a) that the shift from carboxylate to pyrazolate bridging ligands causes a distinct stabilization of low-spin configurations, such that the LLL state is most stable for $[1^3]$ while HHH is most stable for the carboxylate-bridged species. The $M_S = 0$ ground state for the LLL configuration of $[1^3]$ is diamagnetic, with net spin densities of zero: the additional electron is completely delocalized over all three iron centers, and the cluster adopts a perfect D_{3h} -symmetric geometry with Fe-O and Fe-N bond lengths (1.76 Å and 1.96 Å, respectively), very similar to those in the X-ray studies (1.77 Å and 1.94 Å). The calculations therefore reproduce all the key experimental observations: the iron centers in the carboxylate-bridged cluster remain high-spin even after 1-electron reduction while the pyrazolate-bridged analogue favors the low-spin state. A second striking feature is that both intermediate states (HHL and HLL) lie above the dashed line joining the limiting HHH and LLL configurations. They are therefore less stable than the

average and are thermodynamically unstable with respect to a mixture of HHH and LLL, accounting for the absence of detectable intermediate configurations (HHL or HLL). Following Borshch's arguments regarding ligand strain, we can trace the relative instability of the intermediate configurations to patterns in the bond angles and bond lengths summarized in Figure 3(b). The coordination geometries at the Fe centers in the HHH and LLL configurations are typical of isolated high- and low-spin centers: all bond angles are close to 90° and the metal-ligand bond lengths are uniformly shorter in the latter. In the intermediate cases, the coordination geometries around the low-spin centers remain very similar to those in the LLL state, but the high-spin sites are rather distorted with acute O-Fe-N angles of 81° in each case. Thus, it appears that the combination of high- and low-spin centers in a single cluster leads to structural stress, which accumulates around the high-spin centers. The fact that the high-spin centers are the loci of the distortion is a consequence of the absence of ligand-field stabilization, which leads to a rather flexible coordination environment. In contrast, the substantial ligand-field stabilization available to low-spin Fe^{3+/2+} places a high premium on near-perfect octahedral coordination, and as a result the coordination environment is relatively inflexible.

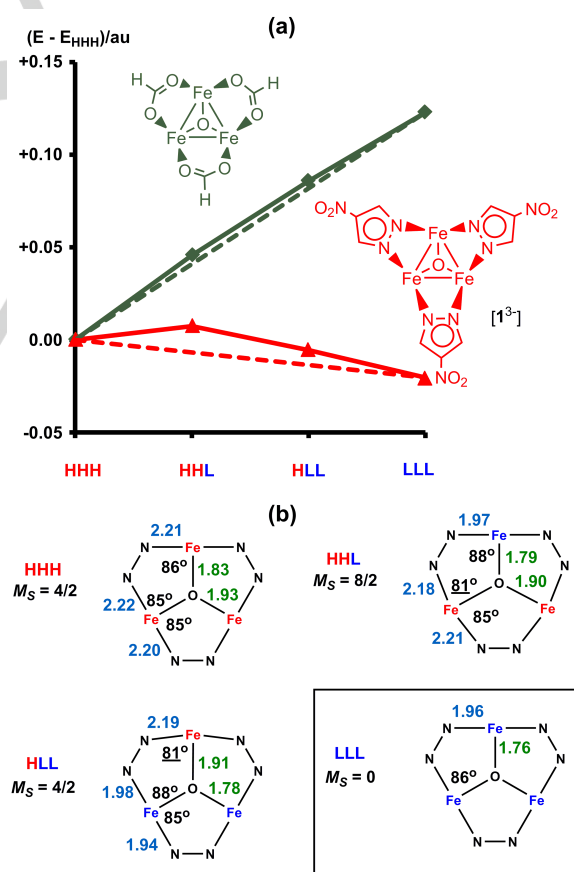


Figure 3. (a) Energies of HHH, HLL, HHL and LLL configurations for $[1^3]$ and its carboxylate-bridged analogue. (b) Structural parameters for the various configurations of $[1^3]$. Bond lengths are color-coded: Fe-O green, Fe-N(pz) blue. All results are obtained using the OPBE functional.

In summary, the trinuclear cluster $[\text{Fe}_3(\mu_3\text{-O})(\mu\text{-4-NO}_2\text{-pz})_6(\text{NCS})_3]^{2-}$ has been synthesized in two distinct oxidation states that have dramatically different electronic configurations. Mössbauer, UV/Vis and vibrational spectroscopies, along with X-ray crystallographic characterization, suggest that all three Fe centers are in locally high-spin configurations at the all-ferric oxidation level, $[\text{Fe}_3(\mu_3\text{-O})(\mu\text{-4-NO}_2\text{-pz})_6(\text{NCS})_3]^{2-}$ but all three switch to low-spin upon one-electron reduction of the cluster. The reversible one-electron redox event, therefore, triggers a concerted cascade wherein multiple metal centers undergo dramatic changes in electronic structure, which in turn causes a significant change in the effective diameter of the cluster. An electronic structure analysis confirms that the mixed HLL and HLL clusters are thermodynamically unstable with respect to the limiting all-high-spin and all-low-spin forms, and further shows that this instability stems from the incompatibility of high- and low-spin geometries in the same triangular motif.

Experimental Section

$[\text{NBu}_4]_2[\text{Fe}_3(\mu_3\text{-O})(\mu\text{-4-NO}_2\text{-pz})_6(\text{NCS})_3]$, $[\text{NBu}_4]_2[1^{2-}]$. Excess of NH_4SCN (0.155 g; 2.039 mmol) was added to a solution of $[\text{NBu}_4]_2[\text{Fe}_3(\mu_3\text{-O})(\mu\text{-4-NO}_2\text{-pz})_6\text{Cl}_3]$ (0.058 g; 0.040 mmol) in 15 mL of CH_2Cl_2 and the mixture was stirred for 24 h, with a color change from orange-red to deep red. The reaction mixture was filtered and the filtrate was layered with hexane (Yield 0.040 g; 66 %). Anal. Found (Calc.) for $(\text{C}_{53}\text{H}_{84}\text{Fe}_3\text{N}_{23}\text{O}_{13}\text{S}_3)$: C, 41.38 (42.01); H, 5.55 (5.59); N, 21.52 (21.26). **$[\text{NET}_3\text{H}]_2[\text{Fe}_3(\mu_3\text{-O})(\mu\text{-4-NO}_2\text{-pz})_6(\text{NCS})_3] \cdot 4\text{CH}_2\text{Cl}_2$, $[\text{NET}_3\text{H}]_2[1^{2-}]$.** was similarly synthesized starting from $[\text{NET}_3\text{H}]_4[\text{Fe}_3(\mu_3\text{-O})(\mu\text{-4-NO}_2\text{-pz})_6\text{Cl}_3]\text{Cl}_2$.^[2] X-ray quality crystals of $[\text{NET}_3\text{H}]_2[1^{2-}]$ have been obtained by layering its dichloromethane solution with hexane. **$[\text{NBu}_4]_3[\text{Fe}_3(\mu_3\text{-O})(\mu\text{-4-NO}_2\text{-pz})_6(\text{NCS})_3]$, $[\text{NBu}_4]_3[1^{3-}]$.** Bu_4NBH_4 (0.017 g; 0.066 mmol) was added to a solution of $[\text{NBu}_4]_2[\text{Fe}_3\text{O}(\text{NO}_2\text{pz})_6(\text{NCS})_3]$ (95 mg; 0.063 mmol) in 20 mL of anhydrous CH_2Cl_2 leading to almost immediate color change from red to dark brownish-red. After stirring for 12 h, the product was precipitated by slow Et_2O vapor diffusion into the reaction mixture (Yield 0.088 g; 80 %). Anal. Found (Calc.) for $\text{C}_{69}\text{H}_{120}\text{Fe}_3\text{N}_{24}\text{O}_{13}\text{S}_3$: C, 46.23 (47.15); H, 6.81 (6.88); N, 19.20 (19.13). **$[\text{PPh}_4][\text{CoCp}_2]_2[\text{Fe}_3(\mu_3\text{-O})(\mu\text{-4-NO}_2\text{-pz})_6(\text{NCS})_3] \cdot \text{CH}_2\text{Cl}_2$** ($[\text{PPh}_4][\text{CoCp}_2]_2[1^{3-}]$) was similarly synthesized by using $[\text{PPh}_4]_2[\text{Fe}_3(\mu_3\text{-O})(\mu\text{-4-NO}_2\text{-pz})_6(\text{NCS})_3]$ and CoCp_2 as reducing agent. X-ray quality crystals of $[\text{PPh}_4][\text{CoCp}_2]_2[1^{3-}]$ have been obtained by layering its dichloromethane solution with hexane.

X-ray data for $[\text{NET}_3\text{H}]_2[1^{2-}]$: crystal dimensions 0.60 x 0.60 x 0.10 mm; $T = 210$ K; orthorhombic, space group $P2_12_12$ (No. 18); $a = 14.432(1)$ Å, $b = 18.829(2)$ Å, $c = 12.324(1)$ Å, $V = 3349.0(5)$ Å³, $Z = 2$; $\rho_{\text{calc}} = 1.561$ g cm⁻³; $\mu = 1.124$ mm⁻¹; $6.04 < 2\theta < 53.02$; of 6927 unique reflections, 6554 were observed [$I > 2\sigma(I)$]; 426 parameters; $R_1 = 0.0382$, $wR_2 = 0.1075$ for $I > 2\sigma(I)$; GOF = 1.077. **X-ray data for $[\text{PPh}_4][\text{CoCp}_2]_2[1^{3-}]$:** crystal dimensions 0.20 x 0.06 x 0.02 mm; $T = 100$ K; monoclinic, space group $P2_1/c$ (No. 14); $a = 10.7335(6)$ Å, $b = 25.718(1)$ Å, $c = 26.391(2)$ Å, $\beta = 90.203(2)$ Å, $V = 7279.0(8)$ Å³, $Z = 4$; $\rho_{\text{calc}} = 1.671$ g cm⁻³; $\mu = 1.289$ mm⁻¹; $5.6 < 2\theta < 52.08$; of 14289 unique reflections, 11307 were observed [$I > 2\sigma(I)$]; 1000 parameters (2 restraints); $R_1 = 0.0365$, $wR_2 = 0.0748$ for $I > 2\sigma(I)$; GOF = 1.008. CCDC-1483806 and CCDC-1483807 contain the supplementary crystallographic data for this paper. These data can be obtained free of charge via www.ccdc.cam.ac.uk/conts/retrieving.html (or from the Cambridge Crystallographic Data Centre, 12 Union Road, Cambridge CB21EZ, UK; fax: (+44)1223-336-033; or deposit@ccdc.cam.ac.uk).

Acknowledgements

EVG, IC and RGR acknowledge the financial support of this work by the National Science Foundation, USA (CHE 0822600). KAA acknowledges the financial support of HCED Iraq. YS and JEM acknowledge financial support from the COST Action CM1305 (ECOSTBio).

Keywords: Mixed-valence • trinuclear iron complex • high-spin/low-spin transition • density functional theory • Mössbauer spectroscopy

- [1] H. N. Miras, I. Chakraborty, R. G. Raptis, *Chem. Commun.* **2010**, 46, 2569-2571.
- [2] D. Piñero, P. Baran, R. Boca, R. Herchel, M. Klein, R. G. Raptis, F. Renz, Y. Sanakis, *Inorg. Chem.* **2007**, 46, 10981-10989.
- [3] W. M. C. Sameera, D. M. Piñero, R. Herchel, Y. Sanakis, J. E. McGrady, R. G. Raptis, E. M. Zueva, *Eur. J. Inorg. Chem.* **2012**, 3500-3506.
- [4] R. D. Cannon, R. P. White, *Prog. Inorg. Chem.* **1988**, 36, 195-298.
- [5] C. Wilson, B. B. Ineren, J. Overgaard, F. K. Larsen, G. Wu, S. P. Palli, G. A. Timco, N. V. Gerbeleu, *J. Am. Chem. Soc.* **2000**, 122, 11370-11379.
- [6] A. N. Georgopoulou, Y. Sanakis, V. Psycharis, C. P. Raptopoulou, A. K. Boudalis, *Hyperfine Interact.* **2010**, 198, 229-241.
- [7] R. Wu, M. Poyraz, F. E. Sawrey, C. E. Anson, S. Wocadlo, A. K. Powell, U. A. Jayasooriya, R. D. Cannon, T. Nakamoto, M. Katada, H. Sano, *Inorg. Chem.* **1998**, 37, 1913-1921.
- [8] T. Nakamoto, M. Hanaya, M. Katada, K. Endo, S. Kitagawa, H. Sano, *Inorg. Chem.* **1997**, 36, 4347-4359.
- [9] C.-C. Wu, S. A. Hunt, P. K. Gantzel, P. Guetlich, D. N. Hendrickson, *Inorg. Chem.* **1997**, 36, 4717-4733.
- [10] T. Sato, F. Ambe, K. Endo, M. Katada, H. Maeda, T. Nakamoto, H. Sano, *J. Am. Chem. Soc.* **1996**, 118, 3450-3458.
- [11] C. Stadler, J. Daub, J. Köhler, R. Saalfeld, V. Coropceanu, V. Schünemann, C. Ober, A. X. Trautwein, S. F. Parker, M. Poyraz, T. Inomata, R. D. Cannon, *J. Chem. Soc., Dalton Trans.* **2001**, 3373-3383.
- [12] J. Overgaard, E. Rentschler, G. A. Timco, N. V. Gerbeleu, V. Arion, A. Bousseksou, J. P. Tuchagues, F. K. Larsen, *J. Chem. Soc., Dalton Trans.* **2002**, 2981-2986.
- [13] N. F. Curtis, L. Xin, D. C. Weatherburn, *Inorg. Chem.* **1993**, 32, 5838-5843.
- [14] S. Karmakar, A. Chakravorty, *Inorg. Chem.* **1996**, 35, 1935-1939.
- [15] M. A. Halcrow (Ed.), "Spin-Crossover Materials: Properties and Applications", Wiley, **2013**.
- [16] C. G. Allen, N. S. Hush, *Prog. Inorg. Chem.* **1967**, 8, 357-389.
- [17] M. B. Robin, P. Day, *Adv. Inorg. Chem. Radiochem.* **1967**, 10, 247-422.
- [18] a) J. R. Polam, J. L. Wright, K. A. Christensen, F. A. Walker, H. Flint, H. Winkler, M. Grodzicki, A. X. Trautwein, *J. Am. Chem. Soc.* **1996**, 118, 5272-5276. (b) F. A. Walker, *Coord. Chem. Rev.*, **1999**, 185-186, 471-534. (c) R. Benda, V. Schünemann, A. X. Trautwein, S. Cai, J. R. Polam, C. T. Watson, T. Kh. Shokhireva, F. A. Walker, *J. Biol. Inorg. Chem.* **2003**, 8, 787-801. See also S6.
- [19] D. Zhu, Y. Xu, Z. Yu, Z. Guo, H. Sang, T. Liu, X. You, *Chem. Mater.* **2002**, 14, 838-843.
- [20] a) J. N. Harvey, *Struct. Bond.* **2004**, 112, 151-184. b) M. Swart, *Int. J. Quant. Chem.*, **2013**, 113, 2-7. c) M. Swart, *J. Chem. Theor. Comput.*, **2008**, 4, 2057-2066. d) H. Paulsen, V. Schünemann, J. A. Wolny, *Eur. J. Inorg. Chem.* **2013**, 628-641. e) H. Paulsen, A. X. Trautwein, *Top. Curr. Chem.* **2004**, 235, 197-219. f) A. Ghosh, P. Taylor, *Curr. Opin. Chem. Biol.* **2003**, 7, 113. g) S. Zein, S. A. Borshch, P. Fleurat-Lessard, M. E. Casida, H. Chermette, *J. Chem. Phys.* **2007**, 126, 014105, 1-13. h) M. Kepenekian, V. Robert, B. Le Guennic, C. de Graaf, *J. Comput. Chem.* **2009**, 30, 2327-2333. i) A. Domingo, M. A. Carvajal, C. de Graaf, *Int. J. Quant. Chem.* **2010**, 110, 331-337. j) M. Reiher, O. Salomon, B. A. Hess, *Theor. Chem. Acc.*, **2001**, 107, 48-55. k) K. P. Jensen and J. Cirera, *J. Phys. Chem. A*, **2009**, 113, 10033-10039. l) K. P. Kepp, *Inorg. Chem.*, **2016**, 55, 2717-2727. m) K. P. Kepp, *Coord. Chem. Rev.*, **2013**, 257, 196-209.
- [21] a) J.-M. Mouesca, L. Noodleman, D. A. Case, *Int. J. Quantum Chem.* **1995**, 56, 95-102. b) E. M. Zueva, R. Herchel, S. A. Borshch, E. V. Govor, W. M. C. Sameera, R. McDonald, J. Singleton, J. Krzystek, Z. Trávníček, Y. Sanakis, J. E. McGrady, R. G. Raptis, *Dalton Trans.*, **2014**, 43, 11269-11276.
- [22] J. A. Real, H. Bolvin, A. Bousseksou, A. Dworkin, O. Kahn, F. Varret, J. Zarembowitch, *J. Am. Chem. Soc.* **1992**, 114, 4650-4658.
- [23] S. Zein, S. A. Borshch, *J. Am. Chem. Soc.* **2005**, 127, 16198-16201.

- [24] a) A. Y. Verat, N. Ould-Moussa, E. Jeanneau, B. Le Guennic, A. Bousseksou, S. A. Borshch, G. S. Matouzenko, *Chem. Eur. J.* **2009**, *15*, 10070-10082. b) E. M. Zueva, E. R. Ryabikh, S. A. Borshch, *Inorg. Chem.* **2011**, *50*, 11143-11151. c) E. M. Zueva, E. R. Ryabikh, A. M. Kuznetsov, S. A. Borshch, *Inorg. Chem.* **2011**, *50*, 1905-1913.

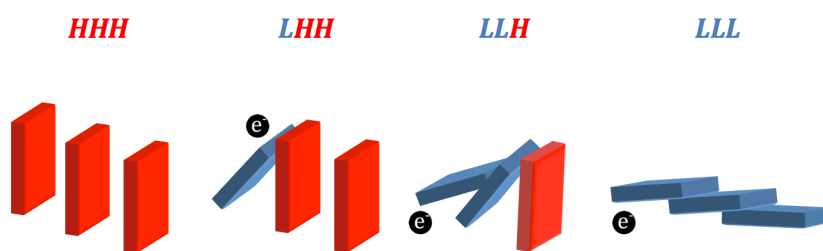
Entry for the Table of Contents

COMMUNICATION

Dr. Evgen V. Govor, Karrar Al-Ameed,
Dr. Indranil Chakraborty, Carla S. Coste,
Olena Govor, Dr. Y. Sanakis,* Prof. John
E. McGrady,* Prof. Raphael G. Raptis*

Page No. – Page No.

**A Redox-Induced Spin-State Cascade
in a Mixed-Valent $\text{Fe}_3(\mu_3\text{-O})$ Triangle**



One-electron reduction flips a trinuclear, all-high spin Fe^{3+} complex to an all-low spin, delocalized $\text{Fe}^{2.66+}$.